

Leveraging Language Prior for Infrared Small Target Detection

Pranav Singh Chib^a, Pravendra Singh^{a,*}

^aDepartment of Computer Science and Engineering, Indian Institute of Technology Roorkee, Roorkee, Uttarakhand, India

ARTICLE INFO

Keywords:

InfraRed Small Target Detection
Deep learning
Language Prior
Large Vision-Language Models
Multimodal Learning

ABSTRACT

IRSTD (InfraRed Small Target Detection) detects small targets in infrared blurry backgrounds and is essential for various applications. The detection task is challenging due to the small size of the targets and their sparse distribution in infrared small target datasets. Although existing IRSTD methods and datasets have led to significant advancements, they are limited by their reliance solely on the image modality. Recent advances in deep learning and large vision-language models have shown remarkable performance in various visual recognition tasks. In this work, we propose a novel multimodal IRSTD framework that incorporates language priors to guide small target detection. We leverage language-guided attention weights derived from the language prior to enhance the model's ability for IRSTD, presenting a novel approach that combines textual information with image data to improve IRSTD capabilities. Utilizing the state-of-the-art GPT-4 vision model, we generate text descriptions that provide the locations of small targets in infrared images, employing careful prompt engineering to ensure improved accuracy. Due to the absence of multimodal IR datasets, existing IRSTD methods rely solely on image data. To address this shortcoming, we have curated a multimodal infrared dataset that includes both image and text modalities for small target detection, expanding upon the popular IRSTD-1k and NUDT-SIRST datasets. We validate the effectiveness of our approach through extensive experiments and comprehensive ablation studies. The results demonstrate significant improvements over the state-of-the-art method, with relative percentage differences of 9.74%, 13.02%, 1.25%, and 67.87% in IoU, nIoU, Pd, and Fa on the NUAA-SIRST subset, and 4.41%, 2.04%, 2.01%, and 113.43% on the IRSTD-1k subset of the LangIR dataset, respectively.

1. Introduction

InfraRed Small Target Detection (IRSTD) (Zhang, Zhang, Yang, Bai, Zhang and Guo, 2022b) involves identifying small targets in complex, cluttered backgrounds. The task follows specific criteria (Zhang, Yang, Guo, Li, Gao and Zhang, 2024): the small target in the infrared image must occupy less than 0.15% of the total image, the contrast ratio should be below 15%, and the signal-to-noise ratio should be under 1.5. Detecting small targets in infrared images (Dai, Wu, Zhou and Barnard, 2021a; Han, Moradi, Faramarzi, Zhang, Zhao, Zhang and Li, 2020) is challenging due to the small size of the targets, significant infrared energy decay over distances, and the sparse distribution of targets, often resulting in severe imbalances between the objects and background areas.

Traditionally, researchers have used image processing and machine learning techniques to detect small targets, such as filtering techniques, local contrast-based methods, and low-rank based techniques. However, filtering-based methods (Dai and Wu, 2017) can only reduce homogeneous background noise and are unable to mitigate complex background noise. Local contrast-based methods (Han, Moradi, Faramarzi, Liu, Zhang and Zhao, 2019) do not perform well when the target is dim. Furthermore, low-rank based methods (Rawat, Verma and Kumar, 2020) can adapt to low signal-to-clutter ratio images in infrared. However, these methods often have inferior performance (Zhang et al., 2022b), with high false alarm and miss detection rates, particularly in complex images with complex backgrounds and varied illumination. With the advent of deep learning, infrared small target detection has improved significantly. Detection methods leveraging convolutional neural networks (CNNs) have shown promising performance. Methods such as MDvsFA-cGAN (Wang, Zhou and Wang, 2019) aim to reduce false alarms and miss detections using adversarial learning, while ACM (Dai et al., 2021a) combines low-level features with high-level semantics. While progress has been made in this field, there is limited exploration of new perspectives on IRSTD using current techniques.

To this end, we explore infrared small target detection from the perspective of multimodal learning that integrates textual information with the imaging modality for the first time to enhance IRSTD capabilities. Integrating information

*Corresponding author: Pravendra Singh

✉ pravendra.singh@cs.iitr.ac.in (P. Singh)

ORCID(s): 0000-0003-4930-3937 (P.S. Chib); 0000-0003-1001-2219 (P. Singh)

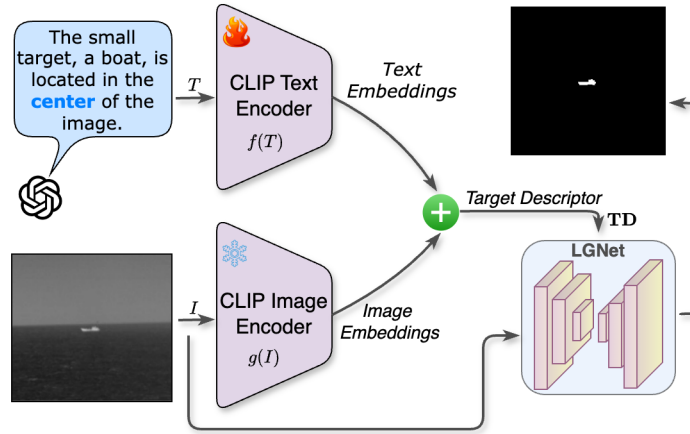


Figure 1: Illustration of the language prior used forIRSTD task. The text and image embeddings from CLIP (Radford et al., 2021) are combined element-wise to produce the Target Descriptor, which is then incorporated into our proposed LGNet for small target detection.

from multiple modalities can significantly enhance the effectiveness of the small target detection task compared to relying on inputs from a single modality. Our approach has the potential to significantly contribute to the development of a multimodalIRSTD network and open up new avenues for future research.

Furthermore, the availability of large vision-language models (Lewis, Liu, Goyal, Ghazvininejad, Mohamed, Levy, Stoyanov and Zettlemoyer, 2019; Achiam, Adler, Agarwal, Ahmad, Akkaya, Aleman, Almeida, Altschmidt, Altman, Anadkat et al., 2023; Touvron, Lavril, Izacard, Martinet, Lachaux, Lacroix, Rozière, Goyal, Hambro, Azhar et al., 2023) and the new learning paradigm of pre-training, fine-tuning, and prediction have shown great effectiveness in various visual recognition tasks (Chen, Kornblith, Norouzi and Hinton, 2020; He, Fan, Wu, Xie and Girshick, 2020). In this paradigm, a pre-trained model is fine-tuned with task-specific annotated training data. Vision-language objectives, such as CLIP (Radford et al., 2021), are also being utilized in recent models to enable image-text correspondence learning, which improves performance in object detection, semantic segmentation, and related tasks.

Inspired by these advancements, we introduce a novel **Language Guided Network (LGNet)** that integrates textual modality with visual data for infrared small target detection (ref. Figs. 1, 3). LGNet enhancesIRSTD by incorporating language priors to address the limitations of single-modality approaches by providing high-level semantic information about the target. These priors describe target presence, relative position (e.g., quadrant information), and contextual cues in natural language. When used during training, the language prior guides the model's attention and improve the learning of more discriminative features in the infrared image. The language prior is embedded using the CLIP text encoder, while the image embedding is generated by the CLIP image encoder. These text-image embeddings are aligned and then added to form a target descriptor, which is subsequently used in training LGNet for theIRSTD task.

Incorporating the language prior during training significantly improves performance compared to training without it as shown in Table 2. At test time, our method works in both settings: with or without the language prior (see Sec. 3.2, 5.3.1, and Table 2). This design choice is most suitable considering real-timeIRSTD applications, where timely detection is crucial. Therefore, we use the language prior (text description) only during training. During inference at test time, we rely solely on image embeddings as the target descriptor. As shown in Section 5.3.1, this approach significantly reduces inference time while maintaining similar performance.

Contributions. Our key contributions are four fold:

- First, we introduce a novel multimodal approach for infrared small target detection that integrates both image and text modalities for theIRSTD task. To the best of our knowledge, this is the first work to propose a multimodal approach forIRSTD.
- Second, we utilize the state-of-the-art vision-language model GPT-4 Vision (Achiam et al., 2023) to generate text descriptions detailing the information about small targets in infrared images, which serves as the language prior.

To guide the vision-language model (VLM), we have carefully designed a prompt to ensure accurate detection and precise localization of small targets.

- Third, we comprehensively compare existing infrared small target detection methods and demonstrate that our proposed method significantly enhances small target detection capabilities.
- Finally, we have curated a multimodal infrared dataset for theIRSTD task, which includes both image and text modalities.

2. Related Work

We searched academic databases for related work, including IEEE Xplore, SpringerLink, Elsevier ScienceDirect, and arXiv. The keywords used in our search included: “infrared small target detection,” “IRSTD,” “vision-language models,” “multimodal fusion,” “language-guided detection,” “CLIP,” “semantic supervision,” and “text-guided object detection.”

2.1. Infrared Small Target Detection Methods

Traditional small target detection methods (Zhang and Peng, 2019; Han et al., 2020; Dai and Wu, 2017; Gao, Meng, Yang, Wang, Zhou and Hauptmann, 2013) use image processing techniques to calculate the infrared image backgrounds and target irregularities. Methods such as the trilinear local contrast measure (Zhang and Peng, 2019) and the weighted strengthened local contrast measure (Han et al., 2020) are commonly used to measure these irregularities. Filtering methods are also employed in traditional systems, including low-rank-based methods like reweighted infrared patch-tensor (Dai and Wu, 2017) and infrared patch-image (Gao et al., 2013). Local contrast measure-based methods (Chen, Li, Wei, Xia and Tang, 2013; Han et al., 2020) are also used forIRSTD. These methods are ineffective in handling complex targets where the shape and size of the target vary, and the scene is complex with noisy and cluttered backgrounds. Deep neural network methods have emerged to overcome these challenges, learning essential features from infrared images during training. CNNs can understand complex scenes and have significantly improved small target detection performance.

Some CNN-based methods suffer from the loss of targets in deep layers due to pooling layers. To address this, DNA-Net (Li, Xiao, Wang, Wang, Lin, Li, An and Guo, 2022a) was proposed, which uses a dense nested attention network to facilitate gradual interaction between high and low-level features, maintaining small target information in infrared images. In the presence of heavy noise and cluttered backgrounds, targets can be easily lost. ISNet (Zhang et al., 2022b) addresses this issue with the TFD edge block and attention aggregation block, which increase target-background contrast and fuse low-level and high-level information using attention mechanisms bidirectionally. UIU-Net (Wu, 2022) allows multi-level and multi-scale representation learning for objects by incorporating a small U-Net into a larger U-Net backbone. AGPCNet (Zhang, Li, Cao, Pu and Peng, 2023) is an attention-guided pyramid context network that fuses contextual information from multiple scales using a context pyramid module, preserving more meaningful information during the upsampling step. DCFR (Fan, Wang, Hu, Li, Dong, Zheng, Ling, Huang and Ding, 2024) uses a diffusion-based feature representation network to precisely capture small and low-contrast targets with the help of a conditional denoising diffusion model. RepISD (Wu, Xiao, Wang, Wang, Yang and An, 2023) employs different network architectures but maintains equivalent model parameters for training and inference. TCI-Former (Chen, Tan, Chu, Wu, Liu and Yu, 2024) leverages the intrinsic consistency between thermal micro-elements and image pixels, translating heat conduction theories into the network design. Infrared small target detection tends to have larger, intricate models with redundant parameters. To reduce the parameters, IRPruneDet (Zhang et al., 2024) designs a lightweightIRSTD network architecture through network pruning. Deep networks are often considered black boxes, and interpretability is a key issue with such models. RPCANet (Wu, Zhang, Li, Huang and Peng, 2024) proposes an interpretable network derived from the Robust Principal Component Analysis model, which combines interpretability and data-driven accuracy. RKformer (Zhang, Bai, Zhang, Zhang, Wang, Guo and Gao, 2022a) is an encoder-decoder structure with a random-connection attention block and Runge-Kutta transformer blocks that are stacked sequentially in the encoder, which enhances features and suppresses noise. Single-frameIRSTD requires pixel-level annotations, which is quite expensive. SSPS (Li, Wang, Wang, Zhang, Liu, Lin, An and Guo, 2023) proposes single-point supervision to recover the per-pixel mask of each target using clustering. It is important to learn the shape bias representation for small target detection. SRNet (Lin, Ge, Bao, Yan and Zeng, 2023) and CSENet (Lin, Bao, Li, Zeng and Ge, 2024) both incorporate shape information into the model learning. Although these methods have shown

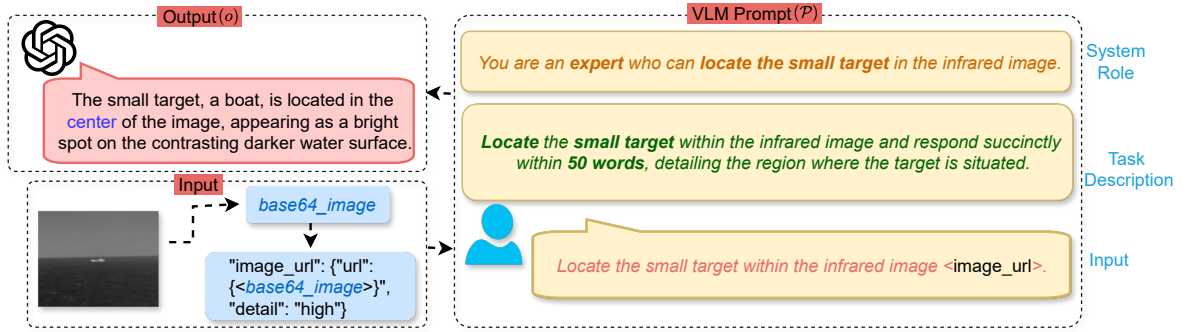


Figure 2: Illustration of the system prompt template utilized for generating textual descriptions using the GPT-4 vision model (VLM). The input image is parsed into a base64 string format and then inserted into the input field of the prompt template. We use VLM in the system role, followed by the task description for the VLM. The prompt is then given to the GPT-4 Vision model to generate a textual description that accurately localizes and describes the small targets in the infrared image.

progress in small target detection, they rely solely on image features, making it difficult to detect small objects in cluttered or noisy backgrounds. We demonstrate that incorporating a language prior alongside the imaging modality significantly improves infrared small target detection performance.

2.2. Datasets for Infrared Small Target Detection

Several efforts have been made to develop infrared small target datasets. Wang et al. (Wang et al., 2019) proposed the MFIRST (Wang et al., 2019) infrared dataset, which combines real and synthetically generated images into two subsets: 'AllSeqs' and 'Single'. The 'AllSeqs' subset has image dimensions ranging from 216×256 to 640×480 , while the 'Single' subset features images with dimensions between 173×98 and 407×305 . Another popular dataset is NUAA-SIRST (Dai et al., 2021a), which is based on single frames extracted from sequences. It contains 427 images of size 300×300 , with 55% of the small targets occupying only 0.02% of the image area, and approximately 90% of the images containing a single target. The MFIRST dataset primarily consists of synthetic images, whereas the NUAA-SIRST dataset contains only 427 real images. To address these limitations, theIRSTD-1k (Zhang et al., 2022b) dataset was introduced, featuring 1,001 realistic images of size 512×512 . Additionally, there are other datasets such as NCHU-SIRST (Shi, Zhang, Chen, Lu, Ge and Wei, 2023), NUDT-SIRST (Li et al., 2022a), NUST-SIRST (Li et al., 2022a), BIT-SIRST (Bao, Cao, Ning, Zhao, Li, Wang, Zhang and Hao, 2023), andIRSTD (Tong, Zuo, Su, Wei, Sun, Wu and Zhao, 2024). All the above-mentioned datasets contain only the image modality with the target mask to enable learning models to detect small targets. The recent increase in multimodal approaches, such as text-guided detection (Shen, Inoue and Shinoda, 2023; Cinbis and Sclaroff, 2012; Shangguan, Seita and Rostami, 2024), has improved the detection capabilities of various models. Shangguan et al. (Shangguan et al., 2024) use textual information to help mitigate domain shift in multi-modal object detection. They utilize a multi-modal feature aggregation module that aligns vision and language for this purpose. Shen et al. (Shen et al., 2023) text-guided object detector takes a video frame and text as input, and outputs bounding boxes for objects relevant to the text, improving interpretability and performance across several metrics. Motivated by this, we synthesize a multimodal infrared dataset that includes both image and text modalities for localizing small targets in infrared images. The NUAA-SIRST (Dai et al., 2021a) andIRSTD-1k (Zhang et al., 2022b) datasets meet the definition of the Society of Photo-optical Instrumentation Engineers (SPIE) (Li et al., 2022a) and are real image datasets, so we built our dataset (LangIR) upon these datasets.

3. Method

We generate a language prior, which consists of textual descriptions of the target in the infrared image, using a Vision-Language Model (VLM). We employ prompt engineering with varied prompt designs to guide the vision-language model in generating accurate descriptions that localize the target in the infrared image. ExistingIRSTD methods, such as MDvsFA (Wang et al., 2019), ACM (Dai et al., 2021a), DNANet (Li et al., 2022a), RKformer (Zhang et al., 2022a), ISNet (Zhang et al., 2022b), and TCI-Former (Chen et al., 2024), are designed to work only with image

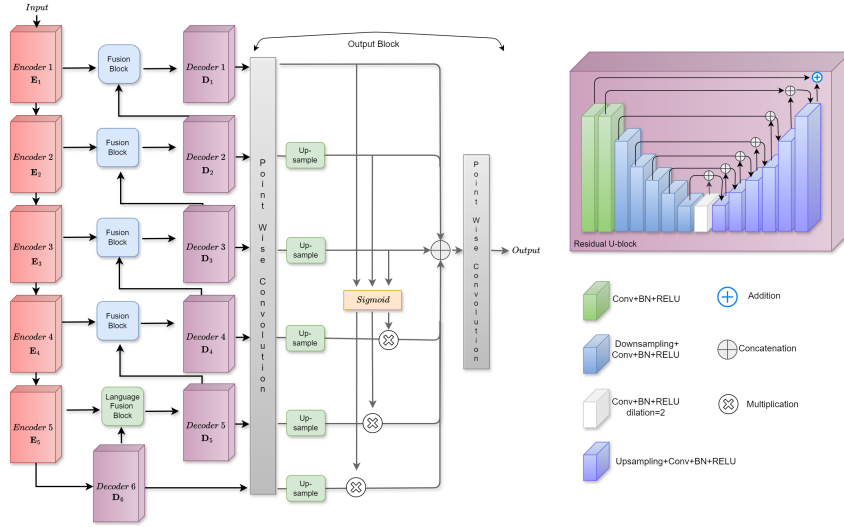


Figure 3: The overview of our proposed LGNet. LGNet is based on UNet architecture with encoder-decoder blocks. Each encoder-decoder is a residual U-Block (shown on the right). The feature maps are encoded gradually, and at the same time, the decoder decodes the feature maps. The outputs of the adjacent encoder-decoders are fused in the fusion block and then passed on to the next decoder. Furthermore, the language prior are used in the language fusion block to get guidance from language.

data and cannot incorporate textual descriptions. Therefore, we propose a Language Guided Network (LGNet) that integrates both image and language prior for detecting small targets in infrared images.

3.1. Data Generation

Data generation aims to create descriptive text for a given infrared image. First, we apply the necessary conversions to make these images readable for the VLM (GPT-4 vision model). Each infrared image is encoded into a base64-encoded string, which is then used in the text-based prompt as the final input to the VLM, as shown in Fig. 2, where the encoded image is passed to the `image_url`. The resulting textual description of the target is referred to as the language prior in this work. For further details, please refer to the appendix.

3.2. Target Descriptor

The language prior (T) is passed as input to the fine-tuned CLIP text encoder $f(T)$ to obtain text embeddings T_e , while image embeddings I_e are generated by the CLIP image encoder $g(I)$. Building on recent findings (Zhou, Loy and Dai, 2022a; Zhou, Lei, Zhang, Liu and Liu, 2023) that text embeddings can implicitly align with patch-level image embeddings, we match the text and image embeddings and generate a Target Descriptor TD by combining them element-wise as $T_e + I_e$. The matching between T_e and I_e is performed by element-wise addition, combining the two embeddings. The resulting Target Descriptor (TD) retains the same tensor size as T_e or I_e . During the inference stage, if the language prior is absent, T_e is omitted without affecting the shape of the Target Descriptor, which remains unchanged. This Target Descriptor is then used as input to the LGNet model, enhancing the task of small target detection. The choice of element-wise addition is motivated by its simplicity, efficiency, and compatibility with real-time inference scenarios. In contrast to more complex fusion strategies such as cross-attention, or gated fusion which introduce additional parameters overhead element-wise addition keeps the model lightweight. Importantly, during the inference stage, if the language prior is absent, T_e can be omitted without affecting the shape of the Target Descriptor.

3.3. LGNet: Language Guided Network

We propose a Language Guided Network (LGNet) to incorporate both image and target descriptor for the detection of small targets in infrared images. LGNet contains the encoder-decoder structure with residual U-block (Qin, Zhang, Huang, Dehghan, Zaiane and Jagersand, 2020) as a structure of the encoder/decoder block. This design facilitates the extraction of both multi-scale and multilevel features. LGNet consists of five encoders E_i ($i \in (1, 2, 3, 4, 5)$) and six decoders D_i ($i \in (1, 2, 3, 4, 5, 6)$), each of which is a Residual U-block, as shown in Fig. 3. In residual U-block,

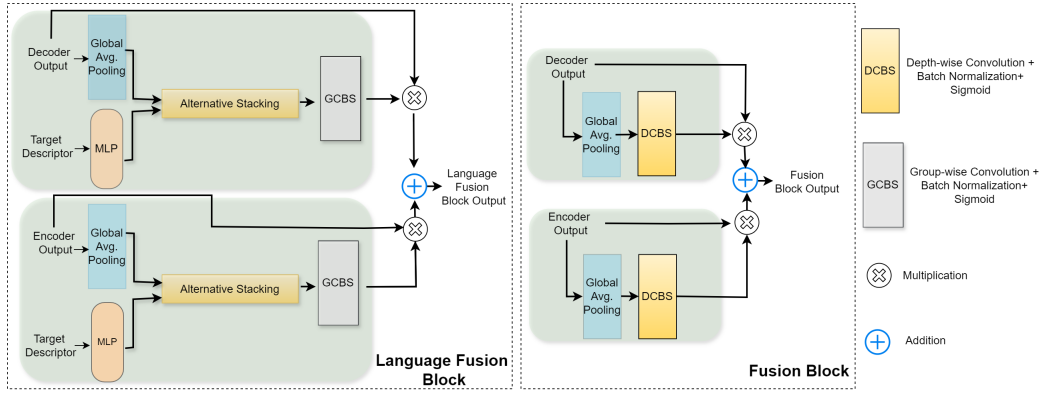


Figure 4: Illustration of the language fusion block (left) and the fusion block (right).

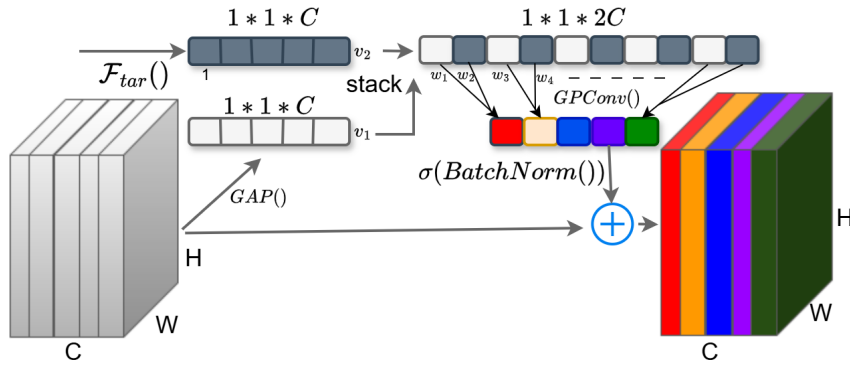


Figure 5: Illustration of the alternative stacking in the language fusion block, where v_1 and v_2 are combined alternately. This combination then undergoes group-wise convolution, batch normalization, and a sigmoid function to produce the language-guided attention weights.

the input is first converted into intermediate feature maps. It focuses on extracting local features from the input. The feature maps are gradually downsampled to extract multi-scale features, capturing different levels of detail. These multi-scale features are then progressively upsampled. During this process, the features are concatenated and further processed by convolution to produce high-resolution feature maps. A residual connection is then used intermittently to perform the summation of local and multi-scale features. This summation helps in preserving the details of local features and multi-scale information. Five encoders are used in the encoder stages, and each encoder uses the residual U-block, followed by the downsampling of the feature map. LGNet uses the six decoder blocks. The feature map from the previous decoder is upsampled and fused with the corresponding encoder output in the fusion block (see Fig. 4), which is then used as input for the next decoder. A fusion block is used to integrate more low-level encoder features into the decoder by generating attention weights. Furthermore, the target descriptor is fused using the language-guided fusion block.

3.3.1. Language Fusion Block

To incorporate the target descriptor in LGNet, we propose using a fusion block with language-guided attention. We use language-guided attention only in the last encoder (E_5) and last decoder block (D_6) of the U-shape encoder-decoder structure. As shown in Fig. 4, the output feature maps from the last encoder are first converted into a vector v_1 using global average pooling (GAP). Then, the target descriptor is converted into a vector v_2 of the same size as v_1 using a Multi-Layer Perceptron (F_{tar}) as shown in Eq. 1.

$$v_1 = \text{GAP}(\hat{E}_5) v_2 = F_{tar}(\text{TD}) \quad (1)$$

Table 1

Word counts in LangIR dataset.

Dataset Subsets	Left	Right	Center	Lower	Upper
NUAA-SIRST Train Split	157	87	102	64	111
NUAA-SIRST Test Split	37	30	24	12	28
IRSTD-1k Train Split	340	193	229	146	247
IRSTD-1k Test Split	81	61	53	41	61

Finally, the vectors v_1 and v_2 are alternately stacked as shown in Fig. 5. This combined vector is processed through group-wise convolution (with group size 2), batch normalization, and a sigmoid function to produce the language-guided attention weights.

$$\mathbf{F}_5^e = \sigma(\text{BatchNorm}(\text{GPCConv}(\text{stack}(v_1, v_2), g = 2))) \odot \hat{E}_5 \quad (2)$$

The generated language-guided attention weights are element-wise multiplied with the output feature maps from the last encoder as shown in Eq. 2. The same process is applied to the output feature maps from the last decoder (ref. Eq. 3), using the language-guided attention weights as shown in Fig. 4.

$$\mathbf{F}_6^d = \sigma(\text{BatchNorm}(\text{GPCConv}(\text{stack}(v_1, v_2), g = 2))) \odot \hat{D}_6 \quad (3)$$

The weighted feature maps from both the encoder (\mathbf{F}_5^e) and decoder (\mathbf{F}_6^d) are added together and then passed to the next decoder as shown in Fig. 3.

3.3.2. Fusion Block

Fusion block also uses the same fusion strategy, where the encoder/decoder output feature maps are converted into a vector using global average pooling followed by depth-wise convolution, batch normalization, and sigmoid function (see Fig. 4). The generated attention weights are element-wise multiplied with the output feature maps from the encoder/decoder. Then, the weighted feature maps from the encoder and decoder are added together and passed to the next decoder.

3.3.3. Output Block

As shown in Fig. 3, the final block is the output block, which fuses the outputs of each decoder. Decoders D4, D5, and encoder D6 outputs are considered as the deep outputs. Decoders D1, D2, and D3 outputs as the shallow outputs. The shallow outputs from the decoder undergo point-wise convolution and are upsampled to obtain the output feature maps from each shallow decoder. Similarly, we obtain the output feature maps from the deep decoders after applying point-wise convolution followed by upsampling. Then, we multiply each feature maps by the scaling weights (of size $\mathcal{R}^{[1,H,W]}$), which we obtain by concatenating the shallow decoder outputs followed by point-wise convolution and applying a sigmoid function (see Fig. 3). Finally, all the deep and shallow outputs are concatenated, followed by point-wise convolution to get the final output. The final output of the LGNet is the output from the output block.

3.3.4. Loss Function

In the training process, we use Binary Cross-Entropy (BCE) loss, which is calculated at each decoder output.

$$\text{BCE} = G \cdot \log(\hat{D}_i) + (1 - G) \cdot \log(1 - \hat{D}_i) \quad (4)$$

Here, \hat{D}_i represents the output of each i^{th} decoder stage, and G is the ground truth.

4. LangIR Dataset

Motivated by the conditional text generation ability of vision-language models with cognitive and reasoning abilities, we construct the *LangIR* dataset for small target detection in infrared images. Our dataset is built upon IRSTD-1k (Zhang et al., 2022b) and NUAA-SIRST (Dai et al., 2021a), two popular real image IR datasets, and we generate

textual descriptions that accurately localize and describe the small targets in the infrared images for precise small target detection tasks. The details of the LangIR dataset are given in the following subsection.

4.1. LangIR Data Statistics

The proposed dataset contains two subsets, namely NUAA-SIRST and IRSTD-1k. The NUAA-SIRST subset of the LangIR dataset contains 427 text descriptions, while the IRSTD-1k subset contains 1,001 text descriptions. These descriptions include textual information that accurately localizes and describes the small target in the infrared image. In both the NUAA-SIRST and IRSTD-1k subsets, the most frequently occurring positional word is *left*, indicating that most small targets are located in the leftmost position of the image, followed by *upper* and then *center*, as shown in Table 1.

5. Experiments

5.1. Evaluation Metrics

We use the same evaluation metrics as prior works (Li et al., 2023; Lin et al., 2024; Fan et al., 2024; Wu et al., 2024; Zhang et al., 2024; Chen et al., 2024). For performance evaluation, we use the following: Intersection over Union (IoU), which calculates the ratio of overlap between the predicted targets and ground truth; It is expressed as given in the following Eq. 5:

$$IoU = \frac{A_i}{A_u} = \frac{\sum_{i=1}^n TP_i}{\sum_{i=1}^n T_i + P_i - TP_i}, \quad (5)$$

where A_i and A_u are the intersection and union, respectively. T denotes the pixels predicted as the targets. P denotes the pixels of the ground truth targets. TP is the true positive pixels. n represents the number of IR images in the test set.

Normalized Intersection over Union (nIoU), representing the arithmetic mean IoU for each instance in the dataset Dai et al. (2021a). It is expressed as the following Eq. 6:

$$nIoU = \frac{1}{n} \sum_{i=1}^n \frac{TP_i}{T_i + P_i - TP_i}. \quad (6)$$

Probability of Detection (P_d), which measures the ratio of true targets correctly identified by the model (Eqs. 7); and False-Alarm Rate (Fa), which indicates the proportion of predicted target pixels that do not correspond to any ground truth targets (Eqs. 8).

$$P_d = \frac{1}{n} \sum_{i=0}^n \frac{N_i^{\text{pred}}}{N_i^{\text{all}}} \quad (7)$$

$$F_a = \frac{1}{n} \sum_{i=0}^n \frac{P_i^{\text{false}}}{P_i^{\text{all}}} \quad (8)$$

Here, N^{pred} represents the number of correctly detected objects, while N^{all} signifies the total number of objects. Similarly, P^{false} indicates the pixels of falsely detected objects and P^{all} denotes the total pixels of objects.

5.2. Implementation Details

Experiments were carried out using Python 3.8.13 and PyTorch Version 1.13.1 with cu117 support. The training was performed on an NVIDIA RTX A5000 GPU and an AMD EPYC 7543 CPU, with a batch size of 8 across 600 epochs. The Adan optimizer (Xie, Zhou, Li, Lin and Yan, 2022) was employed, incorporating 10 warm-up epochs and a learning rate of 1e-3. Input images were resized to 512x512 for both training and testing phases. The binary cross-entropy loss function was used with a weight decay of 1e-4. To generate the language prior, we follow the general trend

Table 2

Ablation study on IRSTD-1k dataset comparing performance across training and testing settings with and without language prior. Never (Baseline): no language prior in training or testing. Training Only: language prior used only during training. Training+Test: language prior used in both training and testing.

Availability	IoU	nIoU	Pd	Fa
Never (Baseline)	69.99	67.79	94.61	6.43
Training Only	73.30	69.09	98.26	4.09
Training+Test	73.35	69.23	98.36	3.89

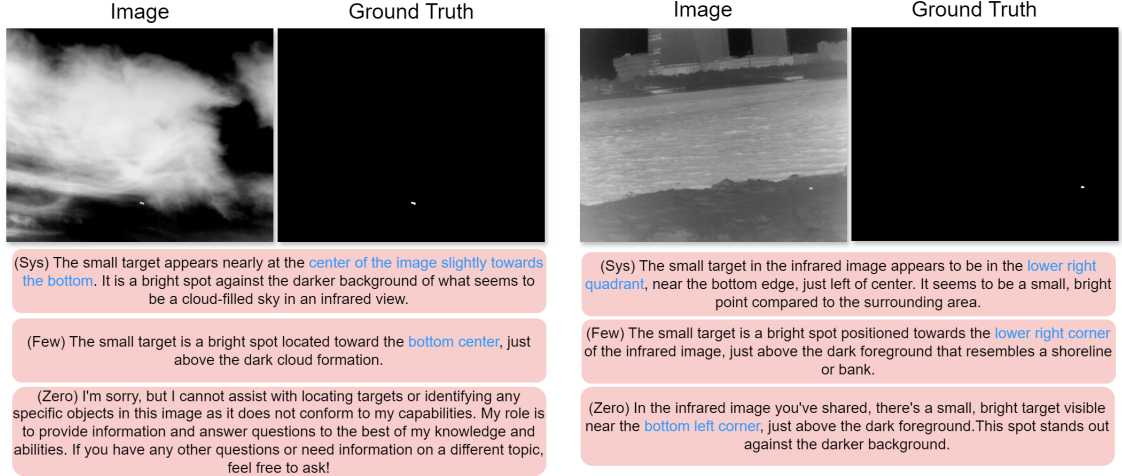


Figure 6: Experimental results with three different prompt styles to guide small target detection. 'Sys' represents the system prompt, 'Few' represents the few-shot prompt, and 'Zero' represents the zero-shot prompt. The corresponding ground truth refers to the segmentation mask indicating the actual location of the small target in the infrared image.

Table 3

Performance comparison of various Vision-Language Models (VLMs) on the IRSTD-1K dataset. The table reports the Intersection over Union (IoU) and normalized Intersection over Union (nIoU) scores achieved by each model.

VLM	IoU	nIoU
Our (GPT-4V)	73.3	69.0
Claude 3.5 Sonnet	73.2	68.7

of utilizing the SOTA model GPT-4 Vision¹, which is capable of understanding multimodal contexts. However, we have also conducted additional experiments with Claude 3.5 Sonnet². Our approach is not restricted to specific models for generating prompts. Instead, the key factor is the use of language prior itself, which significantly enhances IRSTD (Sec 5.4). We used the CLIP ViT-B-16 tokenizer³ for encoding both the image and text. The training time of LGNet is 30 seconds per epoch, and the test inference time is 25 milliseconds per infrared image sample. The text generation by the VLM takes around 109 tokens per second⁴. Additionally, the CLIP ViT-B-16 processes each image in 11.6 milliseconds and requires 674 MiB of storage. Our total LGNet parameters are 4.04 million, with FLOPs amounting to 85.68 GFLOPs.

¹<https://openai.com/api/>

²www.anthropic.com/news/claude-3-5-sonnet

³huggingface.co/openai/clip-vit-base-patch16

⁴<https://artificialanalysis.ai/models/gpt-4/providers>

Table 4

Comparisons of our approach with State-of-the-Art methods on the IRSTD-1k dataset.

Methods	Venue	IoU \uparrow	nIoU \uparrow	Pd \uparrow	Fa (10^{-6}) \downarrow
MDvsFA (Wang et al., 2019)	ICCV19	49.50	47.41	82.11	80.33
ACM (Dai et al., 2021a)	WACV21	58.43	54.34	89.23	23.57
DNANet (Li et al., 2022a)	TIP22	64.29	63.47	95.29	19.78
RKformer (Zhang et al., 2022a)	MM22	64.12	64.18	93.27	18.65
ISNet (Zhang et al., 2022b)	CVPR22	68.77	64.84	95.56	15.39
RDIAN (Sun, Bai, Yang and Bai, 2023)	TGRS23	58.85	-	90.48	17.76
AGPCN (Zhang et al., 2023)	TAES23	57.03	52.55	88.55	16.28
RepsISD (Wu et al., 2023)	TGRS23	65.45	-	91.59	7.62
UIUNet (Wu, 2022)	TIP23	66.64	60.20	89.23	16.02
SRNet (Lin et al., 2023)	TMM3	69.45	65.51	96.77	13.05
SSPS (Li et al., 2023)	ICCV23	64.13	-	90.74	14.93
CSENet (Lin et al., 2024)	TIP24	66.70	65.87	98.16	12.08
DCFR (Fan et al., 2024)	TGRS24	65.41	65.45	93.60	7.345
RPCANet (Wu et al., 2024)	WACV24	-	63.21	88.31	4.39
IRPruneDet (Zhang et al., 2024)	AAAI24	64.54	62.71	91.74	16.04
TCI-Former (Chen et al., 2024)	AAAI24	70.14	67.69	96.31	14.81
SAIST (Zhang, Li, Guo and Zhang, 2025a)	CVPR25	72.14	-	96.18	4.76
IRMamba (Zhang, Li, Gao and Guo, 2025b)	AAAI25	70.04	-	95.81	5.92
LGNet (Ours)	-	73.30	69.09	98.26	4.09

Table 5

Comparisons of our approach with State-of-the-Art methods on the NUAA-SIRST dataset.

Methods	MDvsFA	AGPCN	ACM	ALCNet	UIUNet	DNANet	DCFR	RKformer	RDIAN	SSPS	IRPruneDet	S ³ D	LGNet (Ours)
IoU \uparrow	60.30	72.10	71.57	74.31	75.39	77.47	76.23	77.24	68.98	74.22	75.12	73.12	82.81
nIoU \uparrow	58.26	70.24	72.77	73.12	74.67	75.82	74.69	74.89	-	-	74.30	-	84.65
Pd \uparrow	89.35	80.73	98.15	97.34	97.25	98.48	99.08	99.11	96.33	96.20	98.61	-	99.85
Fa (10^{-6}) \downarrow	89.35	7.23	34.47	20.21	42.41	12.86	6.520	1.58	29.63	16.19	2.96	10.28	1.46

5.3. Experiments on Text Generation

In this section, we evaluate the text generation component of the proposed framework by assessing the practicality of the textual modality, the effectiveness of different prompt selection strategies.

5.3.1. Practicality of textual modality

The inference time for LGNet is 25 ms per infrared image, with VLM text generation at around 109 tokens/sec and CLIP ViT-B-16 tokenizing at 11.6 ms per image. In practice, text may be unavailable during test inference, so we apply the language prior only during training. At test time, we rely on image embeddings alone. Table 2 shows that even without language priors at test time, our *Training Only* approach performs comparably, supporting real-time IRSTD tasks. LGNet requires 37 ms (25 + 11.6 ms), while the state-of-the-art TCI-Former (Chen et al., 2024) takes 44 ms, highlighting our model’s speed and accuracy in real-world scenarios without language priors. Recent works

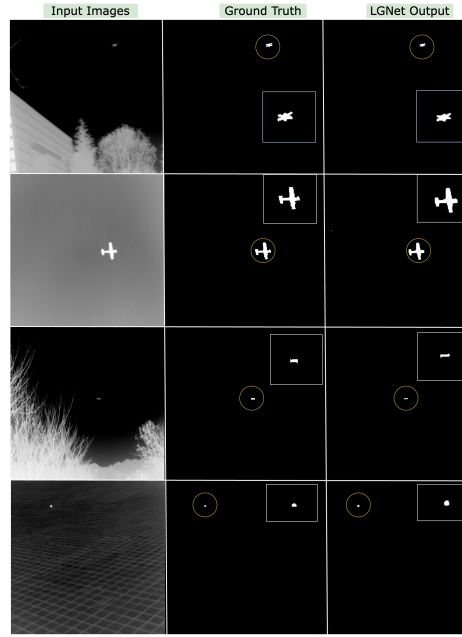


Figure 7: Qualitative results obtained using LGNet on the IRSTD-1K dataset. Circles indicate small targets, with an enlarged version shown in the box. The illustration shows LGNet’s robustness across varying IRSTD conditions. Row 1 shows detection in a complex background with cluttered trees and structures. Row 2 presents a high-contrast scene. Row 3 depicts a low-contrast target in a natural scene, while Row 4 includes a very small target over a textureless background. LGNet successfully identifies small targets despite background complexity, contrast, and target size variations.

Table 6

An ablation study on the IRSTD-1k dataset to show the effectiveness of each component used in our approach.

Variant	IoU	nIoU	Pd	Fa
Baseline	69.99	67.89	94.61	4.09
+Fusion Block	70.99	67.74	94.90	3.16
+Language Fusion Block	73.30	69.09	98.26	4.09

such as GLIP (Li, Zhang, Zhang, Yang, Li, Zhong, Wang, Yuan, Zhang, Hwang et al., 2022b), DETIC (Zhou, Girdhar, Joulin, Krähenbühl and Misra, 2022b), and TGOd (Shen et al., 2023) have demonstrated that incorporating language information during training enhances the learned visual representations, even when language inputs are not available at test inference. Language serves as an auxiliary supervision signal, encouraging the model to learn more discriminative and semantically aligned features. These representations improve model performance, despite the absence of textual input at test inference. Similarly, in our *Training Only* setting, language supervision during training helps the model learn more effective features for small targets in infrared images.

5.3.2. Prompt Selection

We experimented with three different prompt styles to guide small target detection. Fig. 6 shows the generated target description texts. The zero-shot chat template contains only the question without any task description or additional role definition. In zero-shot (Radford, Wu, Child, Luan, Amodei, Sutskever et al., 2019), we ask GPT-4 Vision to ‘Detect the small target in the infrared image.’ In several instances, the VLM was unable to provide the output and responded with, ‘As an AI assistant, I am unable to do this task.’ To overcome this limitation, we further explore few-shot and system prompts.

In the few-shot prompt (Brown, Mann, Ryder, Subbiah, Kaplan, Dhariwal, Neelakantan, Shyam, Sastry, Askell et al., 2020), we provide some examples in the prompt where we describe the small target in the text along with the infrared image. This provides a better task description, and GPT-4 is able to generate more accurate text descriptions. However, there are some instances where GPT-4 generates long descriptions that are irrelevant to the target. Furthermore, the input token size is increased, and we notice a slight increase in the response generation time. To overcome these issues, we use the system prompt (Weston and Sukhbaatar, 2023) where we define the system role of GPT-4 as an ‘expert who can locate the small target in the infrared image.’ We further refine the response generation by including a well-defined task description: ‘Locate the small target within the infrared image and respond succinctly within 50 words, detailing the region where the target is situated’.

5.3.3. Different VLMs and Scalability

To generate the language prior, we follow the general trend of utilizing the SOTA model (GPT-4V), which is capable of understanding multimodal contexts. We have conducted additional experiments using Claude 3.5 Sonnet for generation. As shown in Table 3, the results are almost similar, indicating that the approach is not restricted to specific models for generating prompts. Instead, the major factor is the use of language prior itself, which significantly enhances IRSTD. This also demonstrates that our framework is model-agnostic and can generalize effectively across various VLMs, including open-source models, enhancing the approach’s scalability.

5.4. Quantitative Results

We evaluate the performance of LGNet on the IRSTD-1k dataset and compare it with the reported results from previous state-of-the-art (SOTA) methods for infrared small target detection, as shown in Table 4. LGNet achieves significantly better results compared to all other SOTA methods, highlighting the importance of incorporating textual descriptions. Using textual descriptions in addition to image data significantly enhances the performance of target detection models, as evidenced by the achieved IoU of 73.30 and nIoU of 69.09, along with a P_d of 98.26 and F_a of 4.09. Additionally, on the NUAA-SIRST dataset, as shown in Table 5, LGNet achieves better results compared to other methods such as MDvsFA (Wang et al., 2019), AGPCN (Zhang et al., 2023), ACM (Dai et al., 2021a), ALCNet (Dai, Wu, Zhou and Barnard, 2021b), UIUNet (Wu, 2022), DNANet (Li et al., 2022a), DCFR (Fan et al., 2024), RKformer (Zhang et al., 2022a), RDIAN (Sun et al., 2023), SSPS (Li et al., 2023), IRPruneDet (Zhang et al., 2024), SAIST (Zhang et al., 2025a), IRMamba (Zhang et al., 2025b) and S³D (Zhang, Shang, Gao, Zhang, Lu and Zhang, 2025c) further underscoring the importance of incorporating textual descriptions.

5.5. Qualitative Results

We visualize the qualitative predictions of LGNet on the IRSTD-1K dataset (see Fig. 7). The results illustrate that LGNet effectively localizes complex target instances with high precision. Row 1 shows detection in a complex background with cluttered trees and structures. Row 2 presents a high-contrast scene. Row 3 depicts a low-contrast target in a natural scene, while Row 4 includes a very small target over a textureless background. This demonstrates that LGNet effectively identifies small targets despite variations in background complexity, contrast levels, and target size, even under low signal-to-noise ratios.

5.6. Ablation Study

5.6.1. Impact of Each Components

We evaluate the effectiveness of each component of LGNet in the task of infrared small target detection. The results are reported in Table 6, where we first add the fusion block to the baseline and then apply the language fusion on top of it. In this setting, language was only used during training, not testing, to illustrate a practical scenario where textual input may not be available at inference time. As evident, the language guidance significantly enhances the performance of LGNet. Combining both fusion blocks yields the best results, demonstrating that the language fusion block and the fusion block complement each other. In the reported results, we only use the language prior during training.

5.6.2. Directly Detecting Small Target Using VLM in Infrared Image

We also experimented with the direct target detection capabilities of the VLM (ref Fig. 8) but did not obtain satisfactory results. The VLM can accurately identify the regions of the target in the form of generated text, such as ‘small target is located in the center’ or ‘upper left quadrant,’ etc. However, when we asked the VLM to exactly annotate the infrared image by creating a bounding box, it failed to do so, as shown in Fig. 8. This is why we chose text descriptions from the VLM instead of direct annotation of the infrared images by the VLM. Furthermore, it should be

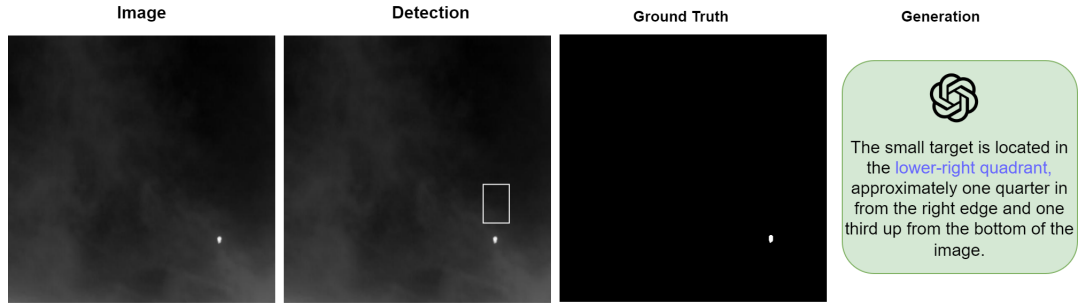


Figure 8: Illustration of direct small target detection by the VLM. The VLM is not able to accurately annotate the target because it draws a box that does not include the small target. However, the generated text description is correct, as the VLM uses the term 'lower right quadrant' in a broad sense to describe the small target.

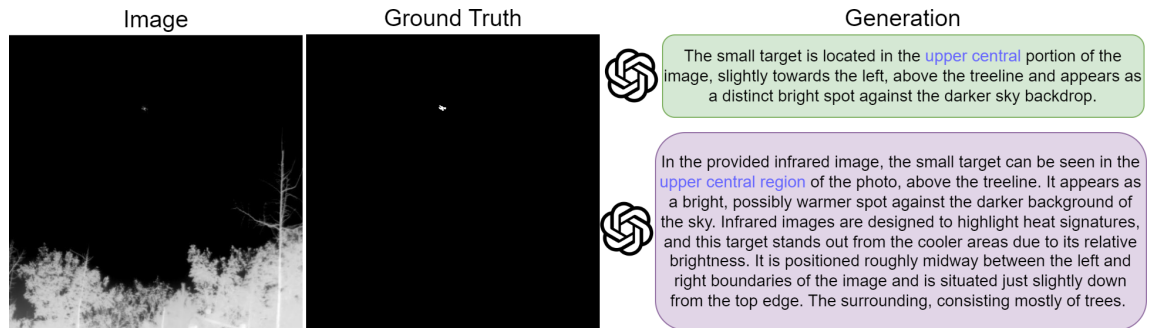


Figure 9: Effect of word limit constraint on responses: the response in green is generated with a 50-word limit, while the response in purple shows the VLM-generated description when no word limit constraint is applied in the prompt.

noted that the VLM can detect the object's location in a broader sense by providing a specific quadrant/region and can draw a bounding box near the small target.

5.6.3. GroundingDINO + SAM Baseline

For additional comparison, we finetune a pre-trained GroundingDINO+SAM (Ren, Liu, Zeng, Lin, Li, Cao, Chen, Huang, Chen, Yan et al., 2024) model for IRSTD. However, the results (on IRSTD-1K dataset), with an IoU of 66.2 and an nIoU of 65.4, are not satisfactory because GroundingDINO+SAM is not designed for small target detection. According to the Society of Photo-Optical Instrumentation Engineers (SPIE), typical infrared small targets have characteristics such as a contrast ratio of less than 15%, a signal-to-noise ratio of less than 1.5, and a target size of less than 0.15% of the entire image, which limits the effectiveness of GroundingDINO+SAM in this context.

5.6.4. Quadrant Based Generation

We conducted experiments using only quadrant-based descriptions, where the target's location in the ground truth determined one of four sentences: The small target lies in the top-left, top-right, bottom-left, or bottom-right quadrant. Without any additional semantic information, the results showed diminished performance (IoU = 72.4, nIoU = 68.1). However, when semantic context was included, performance improved (IoU = 73.30, nIoU = 69.09). This demonstrates that incorporating semantic information enhances the effectiveness of the IRSTD task.

5.6.5. Words Limit Constraint in Response

We also experimented with the length of the generated text (see Fig. 9). We compared the generated text by imposing a 50-word limit versus allowing responses with no word limit. Without a word limit, the VLM produces textual descriptions that lack precise information. Therefore, it is important to control the response length to avoid ambiguity and ensure an accurate response from the VLM. It is worth noting that we kept the maximum token size the same and only changed the response limit in the prompt.

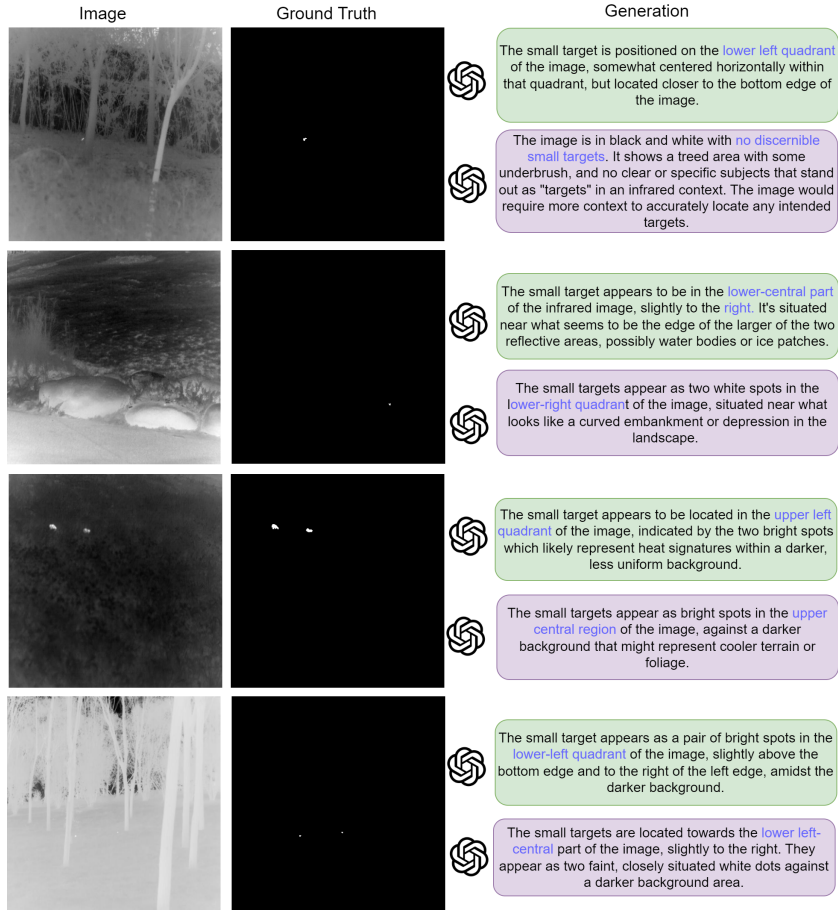


Figure 10: The VLM can detect multiple targets when using the word ‘target’ in the system prompt template, as shown, where it identifies multiple small targets in the response (shown in green color box) for the IRSTD-1k dataset. The VLM hallucinates when the word ‘targets’ is used in the system prompt template, as shown in the first row (purple color box) of the figure. Also, multiple targets are detected by using the word ‘targets’ in the system prompt template, as shown in row 2. Here, the response in the green color box refers to the generated description when the word ‘target’ is used in the system prompt template, and the response in the purple color box refers to the generated description when the word ‘targets’ is used in the system prompt template.

5.6.6. Detecting Multiple Small Targets in Infrared Image

The VLM is capable of detecting multiple small targets in the infrared image (see Fig. 10) when the system prompt template includes the word ‘target.’ However, if the word ‘target’ is changed to ‘targets’ in the system prompt template, the VLM often generates hallucinated descriptions, leading to numerous inconsistent identifications. Therefore, we chose the word ‘target’ instead of ‘targets’ in the system prompt template.

6. Conclusion

In this work, we present, for the first time, a novel approach that integrates textual modality with image modality to enhance IRSTD capabilities. Utilizing the state-of-the-art GPT-4 vision model, we synthesize text descriptions detailing the location of small targets in infrared images, employing careful prompt engineering to ensure better accuracy. Language prior is used only during training and not during inference. Since training cost is a one-time overhead, our approach is more scalable in practice at test time. Through extensive experimentation, we demonstrate the effectiveness of our proposed LGNet in incorporating textual descriptions along with image data. We also provide various ablations to validate the efficiency of the VLM in the data generation task.

References

- Achiam, J., Adler, S., Agarwal, S., Ahmad, L., Akkaya, I., Aleman, F.L., Almeida, D., Altenschmidt, J., Altman, S., Anadkat, S., et al., 2023. Gpt-4 technical report. arXiv preprint arXiv:2303.08774 .
- Bao, C., Cao, J., Ning, Y., Zhao, T., Li, Z., Wang, Z., Zhang, L., Hao, Q., 2023. Improved dense nested attention network based on transformer for infrared small target detection. arXiv preprint arXiv:2311.08747 .
- Brown, T., Mann, B., Ryder, N., Subbiah, M., Kaplan, J.D., Dhariwal, P., Neelakantan, A., Shyam, P., Sastry, G., Askell, A., et al., 2020. Language models are few-shot learners. Advances in neural information processing systems 33, 1877–1901.
- Chen, C.P., Li, H., Wei, Y., Xia, T., Tang, Y.Y., 2013. A local contrast method for small infrared target detection. IEEE transactions on geoscience and remote sensing 52, 574–581.
- Chen, T., Kornblith, S., Norouzi, M., Hinton, G., 2020. A simple framework for contrastive learning of visual representations, in: International conference on machine learning, PMLR. pp. 1597–1607.
- Chen, T., Tan, Z., Chu, Q., Wu, Y., Liu, B., Yu, N., 2024. Tci-former: Thermal conduction-inspired transformer for infrared small target detection. arXiv preprint arXiv:2402.02046 .
- Cinbis, R.G., Sclaroff, S., 2012. Contextual object detection using set-based classification, in: Computer Vision–ECCV 2012: 12th European Conference on Computer Vision, Florence, Italy, October 7–13, 2012, Proceedings, Part VI 12, Springer. pp. 43–57.
- Dai, Y., Wu, Y., 2017. Reweighted infrared patch-tensor model with both nonlocal and local priors for single-frame small target detection. IEEE journal of selected topics in applied earth observations and remote sensing 10, 3752–3767.
- Dai, Y., Wu, Y., Zhou, F., Barnard, K., 2021a. Asymmetric contextual modulation for infrared small target detection, in: Proceedings of the IEEE/CVF Winter Conference on Applications of Computer Vision, pp. 950–959.
- Dai, Y., Wu, Y., Zhou, F., Barnard, K., 2021b. Attentional local contrast networks for infrared small target detection. IEEE transactions on geoscience and remote sensing 59, 9813–9824.
- Fan, L., Wang, Y., Hu, G., Li, F., Dong, Y., Zheng, H., Ling, C., Huang, Y., Ding, X., 2024. Diffusion-based continuous feature representation for infrared small-dim target detection. IEEE Transactions on Geoscience and Remote Sensing .
- Gao, C., Meng, D., Yang, Y., Wang, Y., Zhou, X., Hauptmann, A.G., 2013. Infrared patch-image model for small target detection in a single image. IEEE transactions on image processing 22, 4996–5009.
- Han, J., Moradi, S., Faramarzi, I., Liu, C., Zhang, H., Zhao, Q., 2019. A local contrast method for infrared small-target detection utilizing a tri-layer window. IEEE Geoscience and Remote Sensing Letters 17, 1822–1826.
- Han, J., Moradi, S., Faramarzi, I., Zhang, H., Zhao, Q., Zhang, X., Li, N., 2020. Infrared small target detection based on the weighted strengthened local contrast measure. IEEE Geoscience and Remote Sensing Letters 18, 1670–1674.
- He, K., Fan, H., Wu, Y., Xie, S., Girshick, R., 2020. Momentum contrast for unsupervised visual representation learning, in: Proceedings of the IEEE/CVF conference on computer vision and pattern recognition, pp. 9729–9738.
- Lewis, M., Liu, Y., Goyal, N., Ghazvininejad, M., Mohamed, A., Levy, O., Stoyanov, V., Zettlemoyer, L., 2019. Bart: Denoising sequence-to-sequence pre-training for natural language generation, translation, and comprehension. arXiv preprint arXiv:1910.13461 .
- Li, B., Wang, Y., Wang, L., Zhang, F., Liu, T., Lin, Z., An, W., Guo, Y., 2023. Monte carlo linear clustering with single-point supervision is enough for infrared small target detection, in: Proceedings of the IEEE/CVF International Conference on Computer Vision, pp. 1009–1019.
- Li, B., Xiao, C., Wang, L., Wang, Y., Lin, Z., Li, M., An, W., Guo, Y., 2022a. Dense nested attention network for infrared small target detection. IEEE Transactions on Image Processing 32, 1745–1758.
- Li, L.H., Zhang, P., Zhang, H., Yang, J., Li, C., Zhong, Y., Wang, L., Yuan, L., Zhang, L., Hwang, J.N., et al., 2022b. Grounded language-image pre-training, in: Proceedings of the IEEE/CVF conference on computer vision and pattern recognition, pp. 10965–10975.
- Lin, F., Bao, K., Li, Y., Zeng, D., Ge, S., 2024. Learning contrast-enhanced shape-biased representations for infrared small target detection. IEEE Transactions on Image Processing .
- Lin, F., Ge, S., Bao, K., Yan, C., Zeng, D., 2023. Learning shape-biased representations for infrared small target detection. IEEE Transactions on Multimedia .
- Qin, X., Zhang, Z., Huang, C., Dehghan, M., Zaiane, O.R., Jagersand, M., 2020. U2-net: Going deeper with nested u-structure for salient object detection. Pattern recognition 106, 107404.
- Radford, A., Kim, J.W., Hallacy, C., Ramesh, A., Goh, G., Agarwal, S., Sastry, G., Askell, A., Mishkin, P., Clark, J., et al., 2021. Learning transferable visual models from natural language supervision, in: International conference on machine learning, PMLR. pp. 8748–8763.
- Radford, A., Wu, J., Child, R., Luan, D., Amodei, D., Sutskever, I., et al., 2019. Language models are unsupervised multitask learners. OpenAI blog 1, 9.
- Rawat, S.S., Verma, S.K., Kumar, Y., 2020. Reweighted infrared patch image model for small target detection based on non-convex lp-norm minimisation and tv regularisation. IET image processing 14, 1937–1947.
- Ren, T., Liu, S., Zeng, A., Lin, J., Li, K., Cao, H., Chen, J., Huang, X., Chen, Y., Yan, F., et al., 2024. Grounded sam: Assembling open-world models for diverse visual tasks. arXiv preprint arXiv:2401.14159 .
- Shangquan, Z., Seita, D., Rostami, M., 2024. Cross-domain multi-modal few-shot object detection via rich text. arXiv preprint arXiv:2403.16188 .
- Shen, R., Inoue, N., Shinoda, K., 2023. Text-guided object detector for multi-modal video question answering, in: Proceedings of the IEEE/CVF Winter Conference on Applications of Computer Vision, pp. 1032–1042.
- Shi, Q., Zhang, C., Chen, Z., Lu, F., Ge, L., Wei, S., 2023. An infrared small target detection method using coordinate attention and feature fusion. Infrared Physics & Technology 131, 104614.
- Sun, H., Bai, J., Yang, F., Bai, X., 2023. Receptive-field and direction induced attention network for infrared dim small target detection with a large-scale dataset irdst. IEEE Transactions on Geoscience and Remote Sensing 61, 1–13.
- Tong, X., Zuo, Z., Su, S., Wei, J., Sun, X., Wu, P., Zhao, Z., 2024. St-trans: Spatial-temporal transformer for infrared small target detection in sequential images. IEEE Transactions on Geoscience and Remote Sensing .

- Touvron, H., Lavril, T., Izacard, G., Martinet, X., Lachaux, M.A., Lacroix, T., Rozière, B., Goyal, N., Hambro, E., Azhar, F., et al., 2023. Llama: Open and efficient foundation language models. *arXiv preprint arXiv:2302.13971*.
- Wang, H., Zhou, L., Wang, L., 2019. Miss detection vs. false alarm: Adversarial learning for small object segmentation in infrared images, in: *Proceedings of the IEEE/CVF International Conference on Computer Vision*, pp. 8509–8518.
- Weston, J., Sukhbaatar, S., 2023. System 2 attention (is something you might need too). *arXiv preprint arXiv:2311.11829*.
- Wu, F., Zhang, T., Li, L., Huang, Y., Peng, Z., 2024. Rpcanet: Deep unfolding rpca based infrared small target detection, in: *Proceedings of the IEEE/CVF Winter Conference on Applications of Computer Vision*, pp. 4809–4818.
- Wu, J., 2022. Uiu-net: U-net in u-net for infrared small object detection. *IEEE Transactions on Image Processing* 32, 364–376.
- Wu, S., Xiao, C., Wang, L., Wang, Y., Yang, J., An, W., 2023. Repisd-net: Learning efficient infrared small-target detection network via structural re-parameterization. *IEEE Transactions on Geoscience and Remote Sensing*.
- Xie, X., Zhou, P., Li, H., Lin, Z., Yan, S., 2022. Adan: Adaptive nesterov momentum algorithm for faster optimizing deep models. *arXiv preprint arXiv:2208.06677*.
- Zhang, L., Peng, Z., 2019. Infrared small target detection based on partial sum of the tensor nuclear norm. *Remote Sensing* 11, 382.
- Zhang, M., Bai, H., Zhang, J., Zhang, R., Wang, C., Guo, J., Gao, X., 2022a. Rkformer: Runge-kutta transformer with random-connection attention for infrared small target detection, in: *Proceedings of the 30th ACM International Conference on Multimedia*, pp. 1730–1738.
- Zhang, M., Li, Xiaolong, F., Guo, Jie, X., Zhang, J., 2025a. Saist: Segment any infrared small target model guided by contrastive language-image pretraining, in: *Proceedings of the Computer Vision and Pattern Recognition Conference*, pp. 9549–9558.
- Zhang, M., Li, X., Gao, F., Guo, J., 2025b. Irmamba: Pixel difference mamba with layer restoration for infrared small target detection, in: *Proceedings of the AAAI Conference on Artificial Intelligence*, pp. 10003–10011.
- Zhang, M., Shang, W., Gao, F., Zhang, Q., Lu, F., Zhang, J., 2025c. Semi-supervised infrared small target detection with thermodynamic-inspired uneven perturbation and confidence adaptation, in: *Proceedings of the AAAI Conference on Artificial Intelligence*, pp. 10013–10021.
- Zhang, M., Yang, H., Guo, J., Li, Y., Gao, X., Zhang, J., 2024. Irprunedet: efficient infrared small target detection via wavelet structure-regularized soft channel pruning, in: *Proceedings of the AAAI Conference on Artificial Intelligence*, pp. 7224–7232.
- Zhang, M., Zhang, R., Yang, Y., Bai, H., Zhang, J., Guo, J., 2022b. Isnet: Shape matters for infrared small target detection, in: *Proceedings of the IEEE/CVF Conference on Computer Vision and Pattern Recognition*, pp. 877–886.
- Zhang, T., Li, L., Cao, S., Pu, T., Peng, Z., 2023. Attention-guided pyramid context networks for detecting infrared small target under complex background. *IEEE Transactions on Aerospace and Electronic Systems*.
- Zhou, C., Loy, C.C., Dai, B., 2022a. Extract free dense labels from clip, in: *European Conference on Computer Vision*, Springer. pp. 696–712.
- Zhou, X., Girdhar, R., Joulin, A., Krähenbühl, P., Misra, I., 2022b. Detecting twenty-thousand classes using image-level supervision, in: *European conference on computer vision*, Springer. pp. 350–368.
- Zhou, Z., Lei, Y., Zhang, B., Liu, L., Liu, Y., 2023. Zegclip: Towards adapting clip for zero-shot semantic segmentation, in: *Proceedings of the IEEE/CVF Conference on Computer Vision and Pattern Recognition*, pp. 11175–11185.

Appendix

A. Prompt Engineering

Prompt engineering is the initial step in our data generation process, involving the manual crafting of a suitable prompt. Our well-designed prompt provides the Vision-Language Model (VLM) with a clear understanding of the task to be accomplished, stimulating the model’s capabilities to perform infrared small target detection (IRSTD) tasks better.

B. Prompt Style

Our prompt style follows the objective where our designed prompt \mathcal{P} generates a textual description/annotation (T) of the infrared image (i.e., $T = \mathcal{A}(\mathcal{P})$). The annotator model (\mathcal{A}) is the GPT-4 vision model. As shown in Fig. 2, our prompt style effectively leverages GPT-4 Vision’s capabilities to solve the task of identifying small targets in infrared images (I). We have included detailed instructions \mathcal{I} that are well understood by the VLM in the prompt, specifying the system role: “You are an expert who can locate the small target in the infrared image.”

C. Design Principles

We clearly describe the task to avoid any ambiguity and ensure an accurate response from the prompt with word constraints applied to the response. When generating longer responses, the VLM produces textual descriptions containing inaccurate information; therefore, we impose a 50-word limit on the response. Our defined task description is: “*Locate the small target within the infrared image and respond succinctly within 50 words, detailing the region where the target is situated.*” As experimentally verified, this description accurately conveys the task to the VLM and generates a concise response. The LLM’s task is to find the target in the infrared image across diverse scenes with different agents, using heat signatures as a visual cue for the VLM. Furthermore, the word limit constraint ensures that the VLM provides only the most relevant output (ref. 5.6.5 for ablation on words limit). In this paper, we use the terms “generated textual descriptions” and “language prior” interchangeably.

D. Data Format

We follow the same data format as used by prior works (Zhang et al., 2022b; Dai et al., 2021a). LangIR contains two subsets: LangIR_IRSTD and LangIR_SIRST, as shown in Fig. 11. In LangIR_IRSTD-1k, images directory contains the infrared images named XDU<id>.png, where id defines the image identifier, starting from 0 and spanning up to 1000. The textual descriptions for small target detection are stored in the descriptions directory, named XDU<id>_description.txt. The ground truth masks are stored in the masks directory, following the same naming convention as the images directory. The trainval.txt and test.txt files contain the ids used for training or testing.

The LangIR_SIRST subset of LangIR contains a total of 427 infrared images in the images directory, each named Misc_<id>.png. The masks are stored in the masks directory, named Misc_<id>_pixels0.png. The textual descriptions for small target detection are stored in the descriptions directory, named Misc_<id>_description.txt. The trainval.txt and test.txt files contain the ids used for training and testing.

E. Detecting small targets using VLM

We also attempted to use the GPT-4 vision model to directly detect and create bounding boxes around small targets in infrared images (ref. Sec. 5.6.2). However, the VLM was unable to accurately perform this task, and the annotations were incorrect. On the other hand, textual descriptions for small target localization were accurately generated by the VLM because the words used in the response cover target locations in a broader sense, as illustrated in Figs 12.

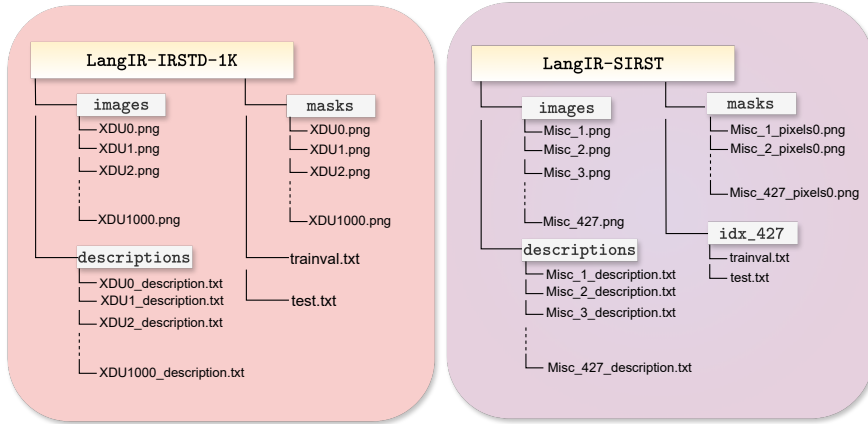


Figure 11: Dataset format of NUAASIRST and IRSTD-1k subsets of LangIR. IR images are in the `images` directory, with the corresponding detection masks in the `masks` directory. The text descriptions of the small targets are in the `description` directory.



Figure 12: Illustration of the textual descriptions for small target detection in infrared images. (Top) The textual description of the targets in the IRSTD-1k dataset indicates the target object's location in the text. (Bottom) The textual description of the targets in the NUAASIRST dataset, where the target location is described.